

Fast and Simple Acquisition of Solid-State ^{14}N NMR Spectra with Signal Enhancement via Population Transfer

Luke A. O'Dell and Robert W. Schurko*

Department of Chemistry and Biochemistry, University of Windsor, 401 Sunset Avenue, Windsor, Ontario N9B 3P4

Received February 18, 2009; E-mail: rschurko@uwindsor.ca

Nitrogen is an element of fundamental importance in almost every aspect of chemistry, yet the 99.6% abundant ^{14}N isotope is not commonly studied by solid-state NMR. This is due in part to its relatively low resonance frequency (28.9 MHz at 9.4 T) but more crucially to its integer spin number ($I = 1$), which results in anisotropic broadening of ^{14}N powder patterns, frequently across several MHz for sites lacking spherical symmetry. This also means that both single-quantum Zeeman transitions are perturbed by the quadrupolar Hamiltonian to first order, and while this interaction can provide valuable information on the local electronic structure, stronger magnetic fields do not reduce the pattern widths. There have been numerous efforts to make solid-state ^{14}N NMR more accessible, and advances have been made in the development of slow sample rotation techniques,^{1,2} overtone spectroscopy,^{3,4} high stability magic angle spinning (MAS),^{5,6} and indirect detection.^{7,8} Each of these methods have associated advantages (sensitivity to dynamics, reduced spectral width, ability to probe chemical shielding anisotropy (CSA), or heteronuclear correlations) and disadvantages (narrow or inefficient excitation, sensitivity to MAS settings, or reliance on coupling to “spy” nuclei), and none of these techniques have become commonplace. In this communication, we show that high-quality static ^{14}N spectra can be obtained at intermediate field strengths in an uncomplicated fashion using frequency-swept pulses, thus allowing the quadrupolar parameters to be accurately measured. Such pulses can increase excitation bandwidths and were first applied to refocus the quadrupolar interaction in integer spins (^2H) by Bodenhausen.⁹ We show that they can be used to exploit the symmetry of integer spin, quadrupolar-dominated powder patterns to achieve signal enhancement via population transfer between the Zeeman levels. This mechanism is demonstrated using numerical simulations and density matrix analysis and confirmed experimentally using a sample of KNO_3 .

Figure 1a shows the ^{14}N powder pattern for KNO_3 (dashed line). The effects of the nitrogen CSA are significantly smaller than the quadrupolar perturbation, so this line shape shows mirror symmetry about the isotropic shift. The two “horns” result from a crystallite orientation in which the largest principal component of the electric field gradient tensor is oriented at an angle $\beta = 90^\circ$ relative to the external field, with one peak for each of the Zeeman transitions as shown. The red outline represents the amplitude profile of a WURST pulse,¹⁰ whose frequency is swept linearly from low to high frequency via modulation of its phase. To observe the effect of this pulse on the $\beta = 90^\circ$ spin system, a $50 \mu\text{s}$ WURST-80 pulse (40 kHz rf power) sweeping from -1.0 to $+1.0$ MHz was simulated using the SIMPSON software,^{11,12} and the density matrix was extracted at three points in time as indicated in Figure 1a. The initial state at time 1 is the density matrix at thermal equilibrium. At time 2 (halfway through the pulse), the $-1 \leftrightarrow 0$ coherence corresponding to the low frequency peak is generated. At this stage a weak $0 \leftrightarrow +1$ coherence is also created, and the population difference between these levels is enhanced, such that once the sweep is completed at time 3, coherences generated between these levels are larger in

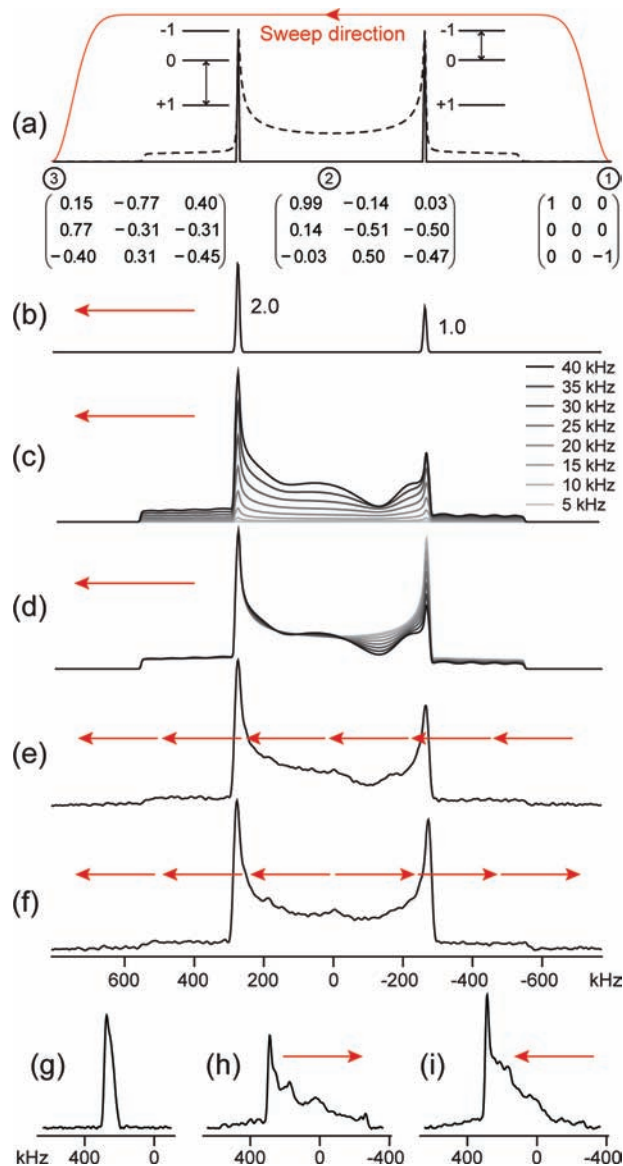


Figure 1. (a) Schematic illustration of a WURST pulse shape (red, not to scale) sweeping across the ^{14}N spectrum of KNO_3 (dashed line, to scale) from right to left. Density matrices are shown for the $\beta = 90^\circ$ crystallite at times 1 (thermal equilibrium), 2 (midpoint of pulse), and 3 (final state). (b) Simulated WURST echo spectrum for the $\beta = 90^\circ$ crystallite with relative intensities shown. (c) Simulations of the KNO_3 powder pattern at different rf field strengths. (d) The same simulations with normalized heights. (e) Experimental spectrum acquired at 9.4 T in 16 pieces with constant sweep direction. (f) Experimental spectrum acquired in 16 pieces with opposite sweep directions on each side of the pattern as shown. (g) A single piece obtained with QCPMG, (h) WURST-QCPMG with incorrect sweep direction, and (i) WURST-QCPMG with correct sweep direction.

magnitude than those of the $-1 \leftrightarrow 0$ transition (significant double-quantum coherences are also generated). The effect of this process on the NMR spectrum is illustrated in Figure 1b, which shows a simulation of a two-pulse WURST echo sequence¹³ on a $\beta = 90^\circ$ crystallite, with the $0 \leftrightarrow +1$ transition showing twice the intensity of the $-1 \leftrightarrow 0$ transition.

This signal enhancement mechanism is similar to DFS,¹⁴ RAPT,¹⁵ or hyperbolic secant¹⁶ methods which have been used to enhance the central transition in half-integer quadrupoles by saturating or inverting satellite transitions. However, the method presented here has two important differences. First, rather than being a “preparatory” sequence added to the start of a standard experiment, the population transfer here is achieved using the same pulses as those which excite and refocus the transverse magnetization; i.e., it is an inherent feature of WURST pulses applied to quadrupolar nuclei, and the effect will occur to some extent whenever a WURST pulse traverses multiple transitions. The second difference is that, for a powder pattern, the population transfer is not applied to a particular transition but to particular crystallite orientations of *each* transition. For example, when the WURST sweep traverses the low frequency side of the KNO_3 powder pattern, it excites the $-1 \leftrightarrow 0$ transition of the $\beta = 90^\circ$ crystallite and the $0 \leftrightarrow +1$ transition of the $\beta = 0^\circ$ crystallite, with corresponding enhancements gained on the opposite transitions on the other side of the pattern.

Figure 1c shows WURST echo simulations of the entire powder pattern. The high frequency side of the spectrum is clearly enhanced, with the enhancement increasing with rf power; however, line shape distortions become apparent at higher power levels. Figure 1d shows these simulations with normalized heights, illustrating clearly that the distortion occurs almost exclusively on the low frequency side. The WURST pulses function over a relatively broad range of rf powers, so the optimum power is therefore a compromise between the extent of signal enhancement and minimization of line shape distortion on the section of the pattern being acquired. Preliminary investigations show that the distortions are dependent on the exact characteristics of the frequency-swept pulses used (i.e., pulse length, amplitude profile, and sweep rate). We are currently investigating this in detail.

Experimental confirmation of the signal enhancement is shown in Figure 1e. This spectrum was acquired on a 5.0 mm static probe at 9.4 T using the recently reported frequency-stepped WURST-QCPMG sequence,^{17,18} with a constant sweep direction for each piece (patterns of width $> ca.$ 500 kHz must be acquired in a piecewise fashion due to the limited probe bandwidth). Sixteen separate pieces were acquired sequentially from high to low frequency at equal intervals of 100 kHz, the innermost pieces centered at ± 50 kHz from the isotropic frequency. A recycle delay of 50 s was used between each scan, with 8 scans per piece (one complete phase-cycle). All 250 frequency-dispersed echoes¹³ recorded in each QCPMG train were coadded before processing, resulting in a spectrum of standard (rather than spikelet) appearance. The high frequency half of the spectrum is clearly enhanced over the low frequency side, and the distortions on the low frequency side closely match the simulations in Figure 1c and d.

To obtain a completely undistorted line shape with enhanced signal on *both* sides, the sweep direction can simply be reversed for the pieces on the low frequency side. The resultant spectrum (Figure 1f) more closely matches the ideal shape. All the discontinuities are clearly visible, and an analytical fit results in a C_Q of 0.75 MHz and $\eta_Q = 0.02$, in agreement with previous studies.^{1,5} The lower frequency “horn” is somewhat reduced in intensity compared with the other, an effect that was observed before in ^{14}N line shapes and explained in terms of equipment-related effects (such as nonoptimal $\lambda/4$ cable length)⁶ which are not accounted

for in the simulations shown here. It may also be partly due to the ^{14}N CSA of $\delta_\sigma = ca.$ 150 ppm in KNO_3 .¹⁹ The slightly increased intensity at the region of the isotropic shift is a result of excitation overlap between the two center-most pieces, which may be reduced by increasing the size of the frequency step.

It is worthwhile noting how quickly the spectrum in Figure 1f was obtained. The total experimental time was under 2 h, in sharp contrast with the times reported for the same spectrum using slow sample rotation by Yesinowski¹ at 7.05 T (four days) or the MAS spectrum obtained by Jakobsen⁵ at 14.1 T (33 h). We note, however, that the MAS method does allow for determination of the ^{14}N CSA parameters,¹⁹ which cannot be precisely measured at 9.4 T using our approach, though they may be obtained at a higher field where the effects of the CSA on the powder pattern are more pronounced. This dramatic improvement in efficiency arises from three sources: (i) the broad excitation bandwidth of the WURST pulses, (ii) the QCPMG protocol, and (iii) the signal enhancement mechanism discussed herein. To quantify their relative contributions, we acquired a single piece near the high frequency “horn” using QCPMG and WURST-QCPMG with both sweep directions. The QCPMG excited a region of only *ca.* 50 kHz width (Figure 1g), with a resultant *S/N* of 79. The increased bandwidth obtained by using WURST pulses is evident from Figure 1h, but the incorrect sweep direction caused distortions and a drop in *S/N* to 64. The enhanced signal obtained with the correct sweep direction (i.e., from low to high frequency for regions on the high frequency side) allowed for both a wide excitation bandwidth and an improved *S/N* of 89 (Figure 1i).

This experiment is equally applicable to other integer spin nuclei such as ^2H ($I = 1$) or ^{10}B ($I = 3$), and the potential enhancement achievable in the latter will be greater given its larger spin number. For this general approach to signal enhancement in integer spin systems, we suggest the acronym DEISM (Direct Enhancement of Integer Spin Magnetization). This work demonstrates that static ^{14}N NMR spectra are easily acquired even at intermediate field strengths, and we hope that it will encourage further studies of this key nucleus.

Acknowledgment. R.W.S. thanks NSERC Canada, the Canadian Foundation for Innovation, the Ontario Innovation Trust, and the University of Windsor for financial support, as well as the Ontario Ministry of Research and Innovation for an Early Researcher Award. L.A.O. thanks DFAIT Canada for a Post-Doctoral Fellowship.

References

- Hill, E. A.; Yesinowski, J. P. *J. Am. Chem. Soc.* **1996**, *118*, 6798–6799.
- Hill, E. A.; Yesinowski, J. P. *J. Chem. Phys.* **1997**, *106*, 8650–8659.
- Bloom, M.; LeGros, M. A. *Can. J. Phys.* **1986**, *64*, 1522–1528.
- Tycko, R.; Opella, S. J. *J. Chem. Phys.* **1987**, *86*, 1761–1774.
- Jakobsen, H. J.; Bildsøe, H.; Skibsted, J.; Giavani, T. *J. Am. Chem. Soc.* **2001**, *123*, 5098–5099.
- Bildsøe, T.; Bildsøe, H.; Skibsted, J.; Jakobsen, H. J. *J. Magn. Reson.* **2004**, *166*, 262–272.
- Gan, Z. *J. Am. Chem. Soc.* **2006**, *128*, 6040–6041.
- Cavadini, S.; Lupulescu, A.; Antonijevic, S.; Bodenhausen, G. *J. Am. Chem. Soc.* **2006**, *128*, 7706–7707.
- Fu, R.; Ermakov, V. L.; Bodenhausen, G. *Solid State Nucl. Magn. Reson.* **1996**, *7*, 1–10.
- Kupče, E.; Freeman, R. *J. Magn. Reson. A* **1995**, *115*, 273–276.
- Bak, M.; Rasmussen, J. T.; Nielsen, N. C. *J. Magn. Reson.* **2000**, *147*, 296–330.
- Tošner, Z.; Vosegaard, T.; Kehlet, C.; Khaneja, N.; Glaser, S. J.; Nielsen, N. C. *J. Magn. Reson.* **2009**, *197*, 120–134.
- Bhattacharyya, R.; Frydman, L. *J. Chem. Phys.* **2007**, *127*, 194503.
- Kentgens, A. P. M.; Verhagen, R. *Chem. Phys. Lett.* **1999**, *300*, 435–443.
- Yao, Z.; Kwak, H. T.; Sakellariou, D.; Emsley, L.; Grandinetti, P. *J. Chem. Phys. Lett.* **2000**, *327*, 85–90.
- Siegel, R.; Nakashima, T. T.; Wasylshen, R. E. *Chem. Phys. Lett.* **2004**, *388*, 441–445.
- O’Dell, L. A.; Schurko, R. W. *Chem. Phys. Lett.* **2008**, *464*, 97–102.
- O’Dell, L. A.; Rossini, A. J.; Schurko, R. W. *Chem. Phys. Lett.* **2009**, *464*, 97–335.
- Giavani, T.; Bildsøe, H.; Skibsted, J.; Jakobsen, H. J. *Chem. Phys. Lett.* **2003**, *377*, 426–432.

JA901278Q